

CrossMark
click for updates

A switch-on MRI contrast agent for noninvasive visualization of methylmercury†

Cite this: DOI: 10.1039/c5cc01723h

Received 27th February 2015,
Accepted 14th June 2015

DOI: 10.1039/c5cc01723h

www.rsc.org/chemcomm

This communication presents the first Gd(III)-based T_1 MRI contrast agent, *o*-MeHgGad, for noninvasive visualization of CH_3Hg^+ . *o*-MeHgGad showed a relaxivity enhancement of 62% in the presence of 1 equiv. of CH_3Hg^+ . Moreover, a noticeable contrast enhancement was recorded in the liver, kidney, and intestine of mice exposed to CH_3Hg^+ . Thus, the newly designed contrast agent has the potential to be used for *in vivo* bio-imaging of CH_3Hg^+ and could be useful for biomedical applications.

Methylmercury (CH_3Hg^+) is a ubiquitous environmental toxicant and a powerful neurotoxicant.¹ Because of its lipid solubility CH_3Hg^+ can readily pass through biological membranes, including the placental barrier during pregnancy.² Therefore, fetuses, infants, and young children are most susceptible to CH_3Hg^+ neurotoxicity with a likelihood of long-lasting neurological and developmental deficits upon exposure to CH_3Hg^+ .³ Consumption of fish and marine mammals is the major source of human exposure to CH_3Hg^+ .⁴ A report from the Food and Agriculture Organization of the United Nations (USFAO) suggests that about one billion people rely on seafood as their primary source of protein (FAO, 2000).⁵ Hence, a large share of the global population is exceedingly vulnerable to CH_3Hg^+ toxicity. Although an array of highly sensitive and specific fluorescent molecular probes has been developed for inorganic mercury (Hg^{2+})⁶ only a few have been investigated as potential CH_3Hg^+ sensors to date.⁷

More recently, a state of the art molecular probe for the selective detection of CH_3Hg^+ in the presence of Hg^{2+} has been reported.⁸ However, fluorescent probes have their own limitation in penetration depth of biological tissues when it comes to *in vivo* imaging.⁹ *In vivo* detection of CH_3Hg^+ becomes even more important when concerned with the prolonged latency periods of CH_3Hg^+ poisoning symptoms after exposure.¹⁰ It is therefore essential to develop an alternative method which can facilitate real-time *in vivo* detection of CH_3Hg^+ for instant diagnosis and for elucidation of CH_3Hg^+ toxicity. Magnetic Resonance Imaging (MRI) has been extensively used for *in vivo* study and is considered to be the safest clinically proven imaging modality for use on patients.¹¹ Gadolinium(III) complexes as extracellular MRI contrast agents have been widely adopted in clinical practice during MRI examinations to enhance the quality of the acquired image. Notably, in recent years, significant advancements have been made in the development of functional MRI contrast agents for molecular imaging of biomolecules. MRI contrast agents for pH,¹² metal ions,¹³ and enzyme activities,¹⁴ have been developed. To our knowledge, no MRI contrast agents for sensing CH_3Hg^+ have been reported.

In this study, we designed and synthesized a new Gd(III)-based turn-on MRI contrast agent, *o*-MeHgGad, for noninvasive visualization of CH_3Hg^+ . The *o*-MeHgGad was obtained through a straightforward and facile synthesis route as shown in Scheme 1. Briefly, the synthesis of *o*-MeHgGad was accomplished in 6 steps. 2-(3-Bromopropoxy)benzaldehyde (**1**) was obtained by reacting 2-hydroxybenzaldehyde with 1,3-dibromopropane. Alkylation of DO3A (tris-*tert*-butyl ester) with compound **1** generated the benzaldehyde derivative of DO3A (tris-*tert*-butyl ester) (**2**). Thiolation of **2** in the presence of $\text{BF}_3 \cdot \text{O}(\text{C}_2\text{H}_5)_2$ gave compound **3**. Subsequent deprotection of compound **3**, first with a solution of dioxin and NaOH (3:1 v/v) and then with 6 N HCl, gave the final ligand (**4**). Metalation of **4** with $\text{GdCl}_3 \cdot 6\text{H}_2\text{O}$ in water at pH 7 followed by HPLC purification yielded *o*-MeHgGad. Additional details of the synthesis of *o*-MeHgGad are provided in the ESI.† In addition, following the synthetic procedure of *o*-MeHgGad, *p*-MeHgGad (*para* derivative) was synthesized and details have been provided in ESI.†

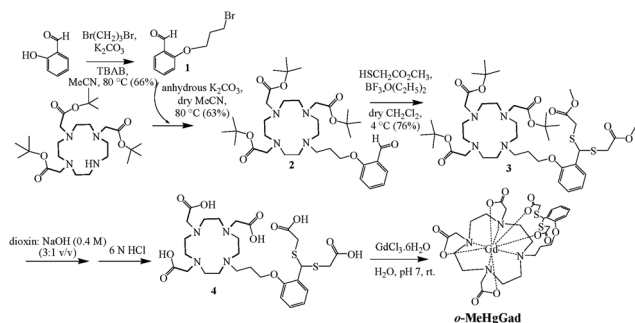
^a Department of Biological Science and Technology, Institute of Molecular Medicine and Bioengineering, National Chiao Tung University, Hsinchu 300, Taiwan.
E-mail: ymwang@mail.nctu.edu.tw; Fax: +886-3-5729288;
Tel: +886-3-5712121 ext. 56972

^b Department of Radiology, Faculty of Medicine, College of Medicine, Kaohsiung Medical University, Kaohsiung, Taiwan

^c Department of Medical Imaging, Kaohsiung Medical University Hospital, Kaohsiung, Taiwan. E-mail: ccy0103@hotmail.com; Fax: +886-7-3154208;
Tel: +886-7-3208235

^d Department of Biomedical Science and Environmental Biology, Kaohsiung Medical University, Kaohsiung 807, Taiwan

† Electronic supplementary information (ESI) available. See DOI: 10.1039/c5cc01723h

Scheme 1 Synthesis of *o*-MeHgGad.

The activation mechanism of *o*-MeHgGad is based on the previously reported Hg^{2+} -promoted elimination of dithioacetal groups¹⁵ and CH_3Hg^+ is expected to show a similar chemical reaction. However, we were a little sceptical about the sensitivity of the reaction due to the less thiophilic nature of CH_3Hg^+ than that of Hg^{2+} .^{7a} Therefore, preliminary investigations towards the proposed chemical reactions leading to activation of the contrast agent were carried out by performing ^1H -NMR of the *o*-MeHgGad ligand in the absence and presence of 3 equiv. of CH_3Hg^+ , under two different solvent systems, dry $\text{DMSO}-d_6$ and D_2O . Noticeable differences in the ^1H -NMR spectra were not observed in the absence or presence of CH_3Hg^+ in dry $\text{DMSO}-d_6$ (Fig. S1, ESI†). On the contrary, significant changes in the spectra were observed in D_2O (data not shown). This prompted us to carry out a concentration dependent ^1H -NMR titration, and the titration spectra are shown in Fig. 1.

As indicated in Fig. 1 a slender shift for the aromatic protons along the downfield was observed in the presence of CH_3Hg^+ . In addition, the peak at 5.3 ppm was found to gradually disappear with the simultaneous appearance of a new singlet at 10.3 ppm with an increasing concentration of CH_3Hg^+ up to 2 equiv. The singlet at 10.3 ppm represents the proton on benzaldehyde formed as a result of the acetylthio elimination in the presence of CH_3Hg^+ . From this study, it can be concluded

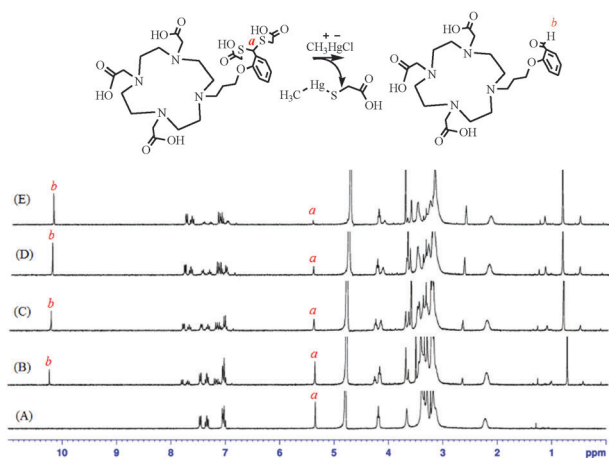


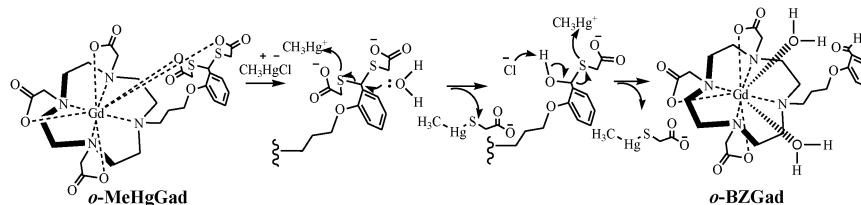
Fig. 1 ^1H NMR spectra (D_2O , 300 MHz) for: (A) *o*-MeHgGad ligand; and (B) 1 : 0.5, (C) 1 : 1, (D) 1 : 1.5, and (E) 1 : 2 mixtures of the *o*-MeHgGad ligand and CH_3Hg^+ .

that CH_3Hg^+ can induce a desulfurization elimination reaction and its mechanism is similar to that observed with inorganic mercury.¹⁵

Next, we evaluated the parameters that influence the contrast enhancement of the $\text{Gd}(\text{III})$ based MRI contrast agent. The efficiency of an MRI contrast agent is assessed in terms of relaxivity (r_1) and the observed relaxivity results from the contribution of the water molecules in the inner and outer coordination spheres.¹⁶ The contribution of metal-bound water molecules to the relaxivity of the $\text{Gd}(\text{III})$ complex is dominant and is referred to as inner sphere relaxivity, given by eqn (1)¹⁶

$$r_1^{\text{IS}} = \frac{qC}{[\text{H}_2\text{O}]} \frac{1}{T_{1\text{M}} + \tau_{\text{M}}} \quad (1)$$

where C represents the molar concentration of the $\text{Gd}(\text{III})$ complex *i.e.*, CA, q is the number of water molecules bound to metal ions, $T_{1\text{M}}$ is the longitudinal relaxation time of the inner-sphere water protons, and τ_{M} is the residence lifetime of the bound water. An obvious inference can be traced from eqn (1): the image intensity can be modulated by altering the q value. In early reports a series of metal responsive MRI contrast agents were developed, which exploit alteration of the hydration state of the $\text{Gd}(\text{III})$ complex.¹⁷ While designing the molecular structure of *o*-MeHgGad we presumed that a pair of appended acetates outside DO3A would saturate the coordination sphere around the $\text{Gd}(\text{III})$ and thereby cease the access of water molecules to the para-magnetic metal centre. However, it is already known that effective interaction between the $\text{Gd}(\text{III})$ and the appended acetate is highly sensitive to the length and flexibility of the linker.¹⁸ Therefore, to decisively determine the coordination status of *o*-MeHgGad, the number of water molecules coordinated directly to the $\text{Gd}(\text{III})$ ion was determined following a previously reported method.¹⁹ The hydration state of *o*-MeHgGad was found to be *ca.* 0.2, which, upon addition of 2 equiv. of CH_3Hg^+ , increased to 1.9 (Table S1, ESI†). The near zero inner sphere coordinated water molecules in *o*-MeHgGad clearly assures that the length and flexibility of the linker is optimal to allow effective coordination of appended acetate to $\text{Gd}(\text{III})$ and further tuning in the structure was not required to achieve complete dormancy of *o*-MeHgGad in terms of water proton relaxivity. To further support the hydration state, the relaxivity of *o*-MeHgGad was determined and it was found to be $2.3 \text{ mM}^{-1} \text{ s}^{-1}$, which is comparable to macrocyclic $\text{Gd}(\text{III})$ complexes with saturated coordination profiles^{13,20} and lower than that of DOTAREM[®] ($q = 1$, Fig. S4, ESI†). The lower relaxivity and saturated coordination sphere of *o*-MeHgGad strongly suggest that it is in a dormant state and it will not reduce the longitudinal relaxation time (T_1) of water protons significantly. In addition, an attempt was made to identify the components of the CH_3Hg^+ triggered hydrolysis of *o*-MeHgGad by FAB mass spectroscopy (Fig. S28, ESI†) and the peaks detected at m/z 663 and m/z 307 support our perceived assertion, which corresponds to *o*-BZGad (refer to Scheme 2) and $\text{C}_3\text{H}_5\text{HgO}_2\text{S}^-$, respectively. Based on these results we envisage and propose the mechanism shown in Scheme 2.



Scheme 2 Systematic representation of the proposed mechanism.

In order to evaluate the practical applicability of *o*-MeHgGad as a CH_3Hg^+ sensor, changes in the relaxivity as a function of CH_3Hg^+ concentration were studied under physiologically simulated conditions. Fig. 2 presents a plot of relaxivity *versus* variable concentrations of CH_3Hg^+ in HEPES buffer (20 mM, pH 7.4). The results presented in Fig. 2 show that an equimolar amount of CH_3Hg^+ evokes 62% gain in the water-proton relaxivity of *o*-MeHgGad, and relaxivity reaches a maximum value of 5.9 (145%) at 3 equiv. of CH_3Hg^+ . The maximum observed relaxivity of *o*-BZGad (refer to Scheme 2) is slightly lower than that of *p*-MeHgGad ($r_1 = 6.4 \text{ mM}^{-1} \text{ s}^{-1}$, Fig. S4, ESI[†]). The difference in the relaxivity of *o*-BZGad and *p*-MeHgGad, which possess an almost similar hydration state ($q \sim 2$), can be justified by taking into account the molecular weights of these two complexes, which are 663 and 813, respectively (Fig. S28, ESI[†]). Moreover, a significant increase in relaxivity was also observed with inorganic mercury ions (Fig. S5, ESI[†]). Only one molar equivalent of inorganic mercury ion is sufficient to elicit an almost $\sim 145\%$ change in relaxivity and this may be a concern regarding the specificity of *o*-MeHgGad toward different mercury species. Nevertheless, it should be noted that 90–100% of the mercury content found in sea foods, especially in fish, is in the form of CH_3Hg^+ . Thus, for the purposes of analysis, any mercury content in fish should be considered CH_3Hg^+ regardless of species as prescribed in an advisory presented by the US Environmental Protection Agency (EPA, 2006).²¹

We further investigated the specificity of *o*-MeHgGad for CH_3Hg^+ by measuring relaxivity changes in the presence of biologically relevant metal ions. Unlike the response observed with CH_3Hg^+ , no noticeable increase in water proton relaxivity of *o*-MeHgGad was observed in the presence of competitive metal ions except Cu(II), as depicted in Fig. 3 (white bar). Upon subsequent addition of 3 equiv. of CH_3Hg^+ to the metal ion

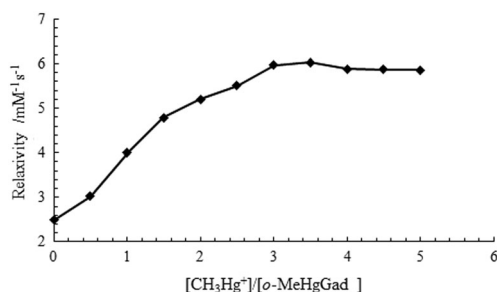


Fig. 2 The relaxivity response of *o*-MeHgGad (0.6 mM) to various concentrations of CH_3Hg^+ at $37.0 \pm 0.1^\circ \text{C}$ and 20 MHz in 20 mM HEPES buffer pH 7.4.

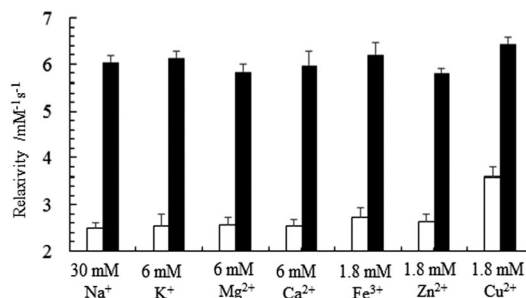


Fig. 3 Relaxivity responses of *o*-MeHgGad to various metal ions. White bars represent the addition of an excess of the appropriate metal ion to a 0.6 mM solution of *o*-MeHgGad. Black bars represent the subsequent addition of 1.8 mM (3 equiv.) CH_3Hg^+ to *o*-MeHgGad. Relaxivity measurements were acquired at $37.0 \pm 0.1^\circ \text{C}$ in 20 mM HEPES buffer (pH 7.4) at 20 MHz.



Fig. 4 CH_3Hg^+ -mediated enhancement of MR images. Images were acquired at 3.0 T (TR/TE = 200/16.3).

containing solutions, relaxivity values approximately similar to those observed for *o*-MeHgGad alone were obtained (black bar), confirming that *o*-MeHgGad is highly selective toward CH_3Hg^+ and the presence of other metal ions does not influence the inherent detection capacity of the *o*-MeHgGad.

Finally, MR imaging studies were carried out to investigate the merits of using *o*-MeHgGad as a CH_3Hg^+ responsive contrast agent. Fig. 4 shows the T_1 -weighted MR images of six Eppendorf tubes. Tubes A and B were controls and contained HEPES buffer (20 mM) and *o*-MeHgGad (0.6 mM), respectively. Tubes C–F contained *o*-MeHgGad (0.6 mM) with CH_3Hg^+ added at 1, 2, 3, and 4 equiv. As can be seen in Fig. 4, solutions of *o*-MeHgGad were visibly darker compared to the complex solution with added CH_3Hg^+ . In addition, gradual intensification in the MRI signal intensity with the increase of the CH_3Hg^+ concentration suggests that *o*-MeHgGad can readily enhance visual differences in CH_3Hg^+ levels. These results are consistent with the relaxivity experiments shown in Fig. 2.

An *in vivo* MR imaging experiment was performed on mice intravenously injected with CH_3Hg^+ (0.1 mmol kg^{-1}) *via* the tail vein. Previous reports on pharmacokinetics and organ distribution of intravenous CH_3Hg^+ in mice suggest elevated retention of CH_3Hg^+ in the liver, kidney, and intestine.²² Therefore, the T_1 -weighted contrast enhancement in the liver, kidney, and

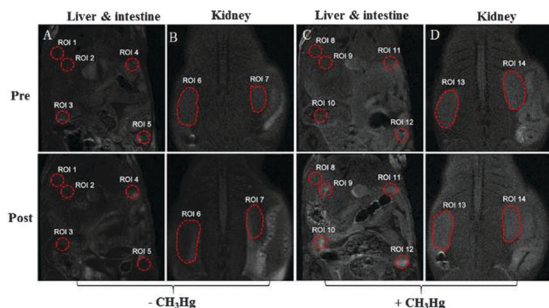


Fig. 5 Representative T_1 -weighted MR images of C57BL/6JNarl mice after injection of *o*-MeHgGad at a dose of 0.1 mmol kg^{-1} . Upper and lower panels show pre-contrast and post-contrast, respectively.

intestine of control and CH_3Hg^+ treated mice was assessed after intravenous injection of *o*-MeHgGad (0.1 mmol kg^{-1}). As can be viewed in Fig. 5A and B, contrast enhancement in the organs under investigation was not observed at 30 min post injection of *o*-MeHgGad in the mice not treated with CH_3Hg^+ . On the contrary, at the same detection time and dose of *o*-MeHgGad, MRI contrast enhancement can be noticed in the liver (Fig. 5C), intestine (Fig. 5C), and kidney (Fig. 5D) of the mice previously intravenously injected with CH_3Hg^+ . For quantitative signal enhancement analysis, fourteen regions of interest (ROI) were drawn manually and contrast enhancement within the ROI was calculated (Table S2, ESI†). Average contrast enhancements of 12, 15, and 22% were recorded in the liver, kidney, and intestine of mice exposed to CH_3Hg^+ , which is higher than the contrast enhancement observed in the control mice (Table S2, ESI†). Taken together, the MR imaging results clearly demonstrate the potential of using *o*-MeHgGad as a MRI contrast agent for the detection of CH_3Hg^+ . Finally, tissue samples from the liver, kidney, and intestine were collected and Gd(III) and Hg(II) ion content in these tissues were analysed by ICP-MS (Table S3, ESI†). A relatively higher concentration of Gd(III) was found in the kidney suggesting that *o*-MeHgGad is filtered and excreted through the kidney.

In conclusion, a newly designed MRI contrast agent was successfully synthesized and characterized for the selective detection of toxic CH_3Hg^+ . The practical usability of *o*-MeHgGad was demonstrated by an *in vivo* MR imaging study on BALB/c nude mice intravenously exposed to CH_3Hg^+ . We believe that the results presented in this report will push the limits of the designed probe towards practical utility in preclinical research endeavours focusing on various aspects of CH_3Hg^+ toxicity.

This work was supported by Ministry of Science and Technology and Ministry of Health and Welfare of the Republic of China for financial support (Health and welfare surcharge of

tobacco products) under contract no. NSC 103-2627-M-009-001, NSC 101-2923-M-009-002, and MOHW 104-TDU-B-212-124-003.

Notes and references

- 1 M. T. Tsui, J. C. Finlay, S. J. Balogh and Y. H. Nollet, *Environ. Sci. Technol.*, 2010, **44**, 6998.
- 2 M. D. Esteban-Vasallo, N. Aragonés, M. Pollan, G. López-Abente and B. Perez-Gomez, *Environ. Health Perspect.*, 2012, **120**, 1369.
- 3 P. Grandjean and K. T. Herz, *Mt. Sinai J. Med.*, 2011, **78**, 107–118.
- 4 C. T. Driscoll, R. P. Mason, H. M. Chan, D. J. Jacob and N. Pirrone, *Environ. Sci. Technol.*, 2013, **47**, 4967.
- 5 J. H. Tidwell and G. L. Allan, *EMBO Rep.*, 2001, **2**, 958.
- 6 (a) M. Santra, B. Roy and K. H. Ahn, *Org. Lett.*, 2011, **13**, 3422; (b) Y. Yan, Y. Zhang and H. Xu, *ChemPlusChem*, 2013, **78**, 628; (c) M. H. Lee, S. W. Lee, S. H. Kim, C. Kang and J. S. Kim, *Org. Lett.*, 2009, **11**, 2101; (d) M. H. Lee, B.-K. Cho, J. Yoon and J. S. Kim, *Org. Lett.*, 2007, **9**, 4515; (e) M. G. Choi, Y. H. Kim, J. E. Namgoong and S. K. Chang, *Chem. Commun.*, 2009, 3560.
- 7 (a) Y. K. Yang, S. K. Ko, I. Shin and J. Tae, *Org. Biomol. Chem.*, 2009, **7**, 4590; (b) M. Santra, D. Ryu, A. Chatterjee, S. K. Ko, I. Shin and K. H. Ahn, *Chem. Commun.*, 2009, 2115.
- 8 Z. Zhang, B. Zhang, X. Qian, Z. Li, Z. Xu and Y. Yang, *Anal. Chem.*, 2014, **86**, 11919.
- 9 S. Mizukami, R. Takikawa, F. Sugihara, Y. Hori, H. Tochio, M. Wächli, M. Shirakawa and K. Kikuchi, *J. Am. Chem. Soc.*, 2008, **130**, 794.
- 10 B. Weiss, T. W. Clarkson and W. Simon, *Environ. Health Perspect.*, 2002, **110**, 851.
- 11 M. G. Shapiro, G. G. Westmeyer, P. A. Romero, J. O. Szabowski, B. Küster, A. Shah, C. R. Otey, R. Langer, F. H. Arnold and A. Jasanoff, *Nat. Biotechnol.*, 2010, **28**, 264.
- 12 S. M. Vibhute, J. Engelmann, T. Verbić, M. E. Maier, N. K. Logothetis and G. Angelovski, *Org. Biomol. Chem.*, 2013, **11**, 1294.
- 13 (a) E. L. Que, E. Gianolio, S. L. Baker, A. P. Wong, S. Aime and C. J. Chang, *J. Am. Chem. Soc.*, 2009, **131**, 8527; (b) E. L. Que and C. J. Chang, *J. Am. Chem. Soc.*, 2006, **128**, 15942.
- 14 (a) J. A. Duimstra, F. J. Femia and T. J. Meade, *J. Am. Chem. Soc.*, 2005, **127**, 12847; (b) S. H. Chen, Y. T. Kuo, G. Singh, T. L. Cheng, Y. Z. Su, T. P. Wang, Y. Y. Chiu, J. J. Lai, C. C. Chang, T. S. Jaw, S. C. Tzou, G. C. Liu and Y. M. Wang, *Inorg. Chem.*, 2012, **51**, 12426; (c) F. Arena, J. B. Singh, E. Gianolio, R. Stefania and S. Aime, *Bioconjugate Chem.*, 2011, **22**, 2625.
- 15 (a) H. Dai, Y. Yan, Y. Guo, L. Fan, Z. Che and H. Xu, *Chem. – Eur. J.*, 2012, **18**, 11188; (b) X. Cheng, S. Li, H. Jia, A. Zhong, C. Zhong, J. Feng, J. Qin and Z. Li, *Chem. – Eur. J.*, 2012, **18**, 1691; (c) X. Cheng, Q. Li, C. Li, J. Qin and Z. Li, *Chem. – Eur. J.*, 2011, **17**, 7276; (d) J. Ros-Lis, M. D. Marcos, R. Martinez-Manez, K. Rurack and J. Soto, *Angew. Chem., Int. Ed.*, 2005, **44**, 4405.
- 16 Y. H. Chang, C. Y. Chen, G. Singh, H. Y. Chen, G. C. Liu, Y. G. Goan, S. Aime and Y. M. Wang, *Inorg. Chem.*, 2011, **50**, 1275.
- 17 E. L. Que and C. J. Chang, *Chem. Soc. Rev.*, 2010, **39**, 51.
- 18 (a) K. D. Verma, A. Forgács, H. Uh, M. Beyerlein, M. E. Maier, S. Petoud, M. Botta and N. K. Logothetis, *Chem. – Eur. J.*, 2013, **19**, 18011; (b) L. M. Matosziuk, J. H. Leibowitz, M. C. Heffern, K. W. MacRenaris, M. A. Ratner and T. J. Meade, *Inorg. Chem.*, 2013, **52**, 12250.
- 19 W. D. Horrocks and D. R. Sudnick, *J. Am. Chem. Soc.*, 1979, **101**, 334.
- 20 M. Polasek and P. Caravan, *Inorg. Chem.*, 2013, **52**, 4084.
- 21 Chapter 12 of the Volunteer Estuary, Monitoring Manual, A. Methods Manual, 2nd edn, EPA-842-B-06-003.
- 22 (a) G. Zareba, E. Cernichiari, L. A. Goldsmith and T. W. Clarkson, *J. Appl. Toxicol.*, 2008, **28**, 535; (b) S. Omata, M. Sato, K. Sakimura and H. Sugano, *Arch. Toxicol.*, 1980, **44**, 231.